Microchimica Acta (2020) 187:649
https://doi.org/10.1007/s00604-020-04608-w

ORIGINAL PAPER

Functionalized Ag/Fe-MOFs nanocomposite as a novel endogenous redox mediator for determination of α2,6-sialylated glycans in serum

Yunfei Zhao[1,2,3] · Jun Chen[1,2,3] · Hangtian Zhong[4] · Chengli Zhang[5] · Yuan Zhou[1,2,3] · Weiran Mao[1,2,3] · Chao Yu[1,2,3]

Received: 8 September 2020 / Accepted: 20 October 2020

Abstract

The development of a novel signal amplification system is described for sensitive determination of α2,6-sialylated glycans (α2,6-sial-Gs), an important prognostic tumor biomarker. First, Fe-based metal-organic frameworks (Fe-MOFs) with silver nanoparticles (AgNPs) decorated onto the outer surface were designed and synthesized with controlled octahedron structures. The new Ag/Fe-MOFs nanocomposite possessed strong conductivity and a large surface area to carry more nanoprobes. To connect the Ag/Fe-MOFs nanocomposite with more groups, the nanocomposite was functionalized by -COOH with SH-PEG-COOH to bind with an α2,6-sial-Gs catcher, M-APBA, via -CONH- bonds. More importantly, the Ag/Fe-MOFs also exhibited an excellent endogenous redox mediator property to produce electrons, which is the fundamental mechanism underlying amplification of an electronic signal. A gold electrode was used to accelerate electron transfer and immobilize the α2,6-sial-Gs lectin (SNA). After the sandwich-type catcher recognition (SNA/α2,6-sial-Gs/M-APBA), the current peak response was provoked in the process of oxidizing AgNPs to Ag^+ in the forward anodic potential sweep, while Cl^- in a PBS solution was transferred into Ag^+ to maintain charge neutrality. Optimized particles were employed for direct fabrication of the sandwich-type affinity biosensor, which was found to show a linear detection range from 1 fg mL^{-1} to 1 ng mL^{-1} with a detection limit of 0.09 fg mL^{-1}. Furthermore, the biosensor exhibited excellent specificity and stability, indicating that such a novel nanobiotechnology platform can be used to initiate potential utility for monitoring biomarkers in serum.

Keywords α2,6-sialylated glycans · Fe-MOFs · Endogenous redox mediator · Electrochemical affinity biosensor · Signal amplification · Silver differential pulse voltammetric signal

Introduction

α2,6-Sialylated glycans (α2,6-sial-Gs) are carbohydrates that mark the growth of carcinoma cells [1]. Overexpression of this tumor marker has been shown to play an important role in the development of tumor progression, such as colon, breast, cervix, and liver cancer [2–5]. Hence, sensitive detection of α2,6-sial-G levels in serum samples is vital for early awareness and clinical management of tumors.

Until recently, high-performance liquid chromatography [6], lectin-based assay, and immunohistochemistry have been used to detect α2,6-sial-Gs [7]. Although these detection methods have the advantages of high analysis accuracy and repeatability, there are some limitations including long analysis time, high cost, cumbersome, laboratory-based, and requiring professional technicians [8, 9]. Thus, developing a sensitive, convenient, and cost-effective method for detecting α2,6-sial-Gs is an urgent need for making clinical decision and providing medical care to patients. Biosensors play an

Yunfei Zhao and Jun Chen contributed equally to this work.

Supplementary Information The online version contains supplementary material available at https://doi.org/10.1007/s00604-020-04608-w.

✉ Chao Yu
yuchaom@163.com

[1] College of Pharmacy, Chongqing Medical University, Box 380#, 1 Yi Xue Yuan Road, Chongqing 400016, People's Republic of China

[2] Chongqing Key Laboratory for Pharmaceutical Metabolism Research, Chongqing 400016, People's Republic of China

[3] Chongqing Pharmacodynamic Evaluation Engineering Technology Research Center, Chongqing 400016, People's Republic of China

[4] School of Public Health, Chongqing Medical University, Chongqing 400016, People's Republic of China

[5] ZiGong First People's Hospital, Zigong 643000, Sichuan, People's Republic of China

Published online: 09 November 2020

important role in the early diagnosis of cancer, due to their superiority in terms of convenience and cost-effectiveness. Various electrode materials have been employed in α2,6-sial-Gs electrochemical sensors in our previous works. For instance, graphene oxide, composites of metal nanomaterials, and carbon-based materials have been used as electrode materials to build sensors [1]. These platforms modified with electron transfer mediators show improved performance; however, we are still seeking for an easier test method with lower detection limit. In this research, we successfully developed a novel α2,6-sial-Gs electrochemical affinity biosensor. Compared to the conventional electrochemical biosensors, the novel biosensor owns a simpler construction route and performs lower detection range than the conventional electrochemical biosensors.

Metal-organic frameworks (MOFs) are class of zeolite-like crystalline porous materials. Their intriguing properties and fascinating structures provide MOFs with the possibility to develop as MOF-based systems [10, 11]. In addition, MOFs carrier can be coated with a large number of nanoparticles due to their high specific surface area [12, 13]. Fe-MIL-88NH_2 is an Fe-based metal-organic frameworks (Fe-MOFs) that has generated considerable interest as a template, because it inherits the advantages of MOFs and possesses excellent biocompatibility [14]. However, the application of MOFs in electrochemical aspect is limited due to their inherent drawbacks, including poor electron transfer capability and unsteadiness in aqueous solution environments [15]. So, combining MOFs with other materials is a reasonable approach to extend the applications of MOFs in sensing fields. For example, PtNPs [16] are embedded within MOFs as scaffolds for aptasensors.

In our study, silver nanoparticles (AgNPs) were introduced to combine with Fe-MOFs, because silver nanoparticles exhibit distinct oxidation peaks in phosphate-buffered saline (PBS) solution as measured by voltammetry [17–19]. However, the current response of the Ag to Ag^+ in PBS solution is too low to achieve high precision and sensitivity detection. In recent years, AgNPs combined with MOFs or metallic oxide system were used as a multifunctional amplifier to catalyze reactions in some researches [20–23]. But as we know, it has not been reported that Ag/MOFs system is an endogenous redox mediator for signal generation. Inspired by the Ag/MOFs amplification system, a novel endogenous redox mediator Ag/Fe-MOFs was synthesized. We believe that the Ag/Fe-MOFs composite can improve the limitation of the two monomers: the one is that this composite have stronger electron transfer capability than Fe-MOFs, and the other is the electrochemical signal generated by Ag/Fe-MOFs in PBS solution is much higher than that of AgNPs alone.

Although Ag/Fe-MOFs produces a synergistic effect, there are still some functional groups, such as –NH_2 and –COOH, which cannot be easily incorporated into Ag/Fe-MOFs during materials synthesis [24]. This defect will affect its connection with biomarkers during the construction of electrochemical sensors, eventually, leading the sandwich structure of the biosensor cannot be formed. The appropriate surface modification is a strategy to provide Ag/Fe-MOFs system with improved analytical performance. SH-PEG-COOH, a linear bifunctional modified PEG, has been widely used to functionalize nanoparticles for drug delivery owing to its unique ability to improve the stability and dispersivity. Interestingly, when Ag/Fe-MOFs doped with SH-PEG-COOH via an Ag-S bond are used to compose a new functionalized endogenous redox mediator (c-Ag/Fe-MOFs), the dispersibility of the resulting composite is improved dramatically. Meanwhile, due to the introduction of –COOH, metal-organic frameworks afford the ability to combine with more functional groups, such as the α2,6-sial-Gs catcher 3-aminophenylboronic acid (M-PABA). After modification of c-Ag/Fe-MOFs with M-PABA (Mc-Ag/Fe-MOFs), a complete signal probe for biosensor was constructed.

In this work, an electrochemical affinity biosensor method was designed successfully by using a gold (Au) electrode and Mc-Ag/Fe-MOFs as the electrochemical signals probe for the first time. The application of the gold electrode provided active sites for the immobilization of α2,6-sial-Gs biotinylated sambucusnigra lectin (SNA) and accelerated the electron transfer rate to improve the sensitivity of the biosensor. Subsequently, the electrode was blocked with bovine serum albumin (BSA). Moreover, to realize the ultrasensitive detection of α2,6-sial-Gs, Mc-Ag/Fe-MOFs were used as a signal probe, which produces electrons via redox reaction between Ag and PBS. With the increased concentration of α2,6-sial-Gs, the differential pulse voltammetry (DPV) signal current peak was found to show a linear upward trend. Thus, a novel sandwich-type affinity biosensor with lower detection limit and simpler construction mode was fabricated (Scheme 1).

Experimental

Materials and chemicals

Dimethylformamide (DMF), $FeCl_3 \cdot 6H_2O$, silver nitrate ($AgNO_3$), ascorbic acid (AA), methylene dichloride (CH_2Cl_2), 3-aminophenylboronic acid (M-APBA), glacial acetic acid, hyaluronic acid, and glucose were obtained from Aladdin (Shanghai, China, www.aladdin-e.com). 2-Aminoterephthalic acid, chitosan, N-hydroxysuccinimide (NHS), N-(3-dimethylaminopropyl)-N-ethylcarbodiimide hydrochloride (EDC), and chondroitin sulfate and hyaluronic acid were purchased from Sigma-Aldrich (St. Louis, USA, www.sigmaaldrich.com). Heparin was obtained from Solarbio (Beijing, China, http://www.solarbio.com/). Biotinylated sambucusnigra lectin (SNA) was purchased from Vector Laboratories, Inc. (USA, Burlingame, www.

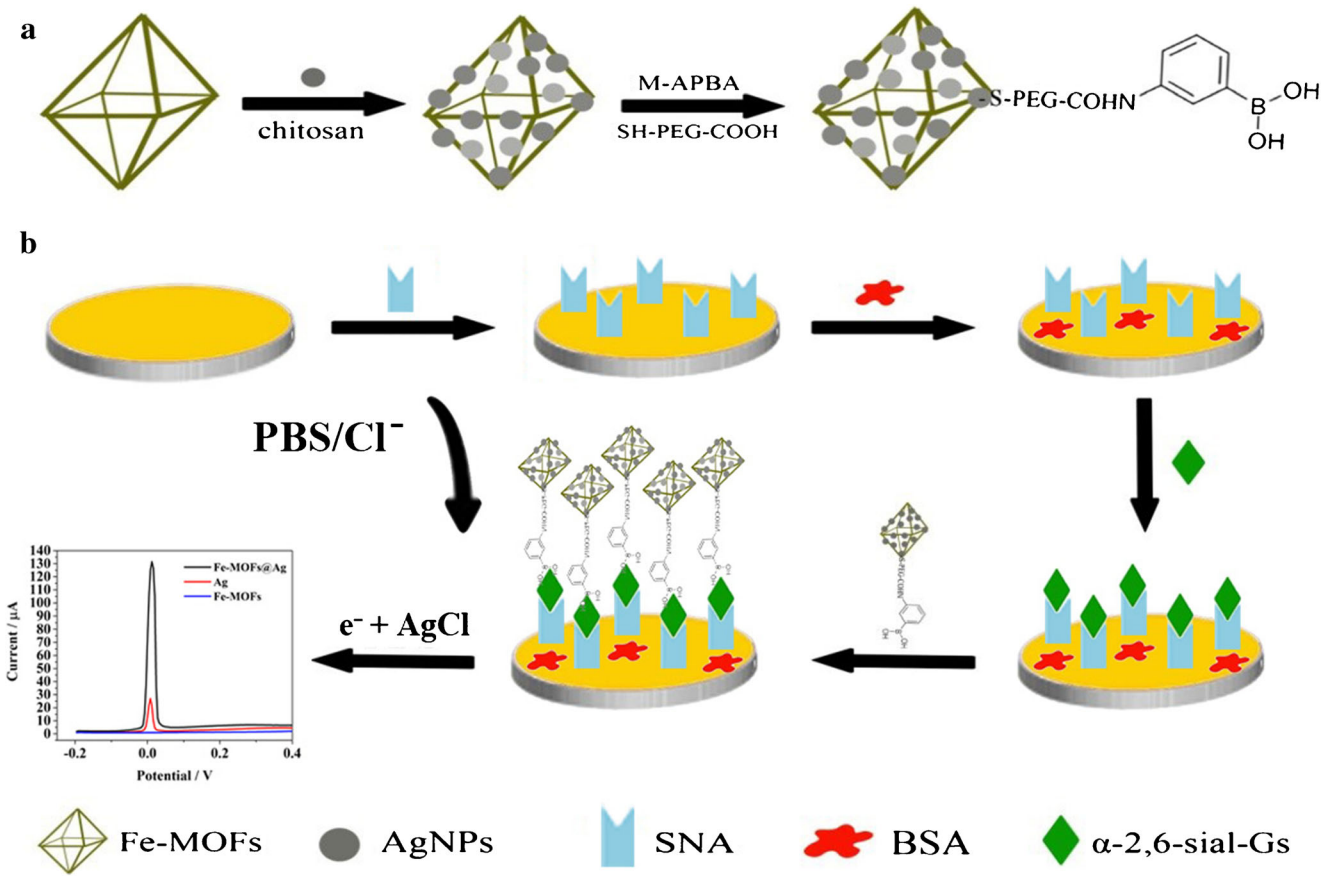

Scheme 1 (A) Preparation process used for the c-Ag/Fe-MOFs/M-PABA. (B) Schematic illustration of biosensor fabrication and electrochemical detection of α2,6-sialylated glycans

vectorlabs.com). Bovine serum albumin (BSA), potassium ferricyanide ($K_3Fe(CN)_6$), and potassium ferrocyanide ($K_4Fe(CN)_6$) were provided by the Beijing Chemical Reagents Company (Beijing, China, www.crc-bj.com). Trisodium citrate dihydrate was purchased from Chengdu KeLong Chemical Group (Chengdu, China, webmaster53029.company.lookchem.cn). SH-PEG_{2000}-COOH was acquired from Xi'an ruixi Biological Technology (Xi'an, China, www.ruixibiotech.com). Neu5Ac α(2–6)Gal β MP and Neu5Ac α(2–3)Gal β MP glycoside were gained from Tokyo Chemical Industry. The phosphate-buffered solution (PBS) was prepared with KCl and H_3PO_4 (pH = 7.2). Ultrapure water (> 18.2 MΩ) obtained from a Millipore Mill-Q purification system was used as the aqueous solution for all the experiments. The serum samples were provided by the University-Town Hospital of Chongqing Medical University (Chongqing, China).

Apparatus and measurements

All electrochemical experiments were performed with a CHI 660D workstation (Chenhua Instruments Co, Shanghai, China) at room temperature. A three-electrode system was used for all the electrochemical measurements, consisting of a platinum wire electrode as the auxiliary electrode, gold electrode (4 mm in diameter) as the working electrode, and a saturated calomel electrode (SCE) as the reference electrode. The images of different nanomaterials were characterized by field emission scanning electron microscopy (FE-SEM, JEOL JSM-6700F, Japan) and transmission electron microscopy (TEM, Hitachi-7500158). UV-Vis absorption spectra were obtained from a UV-2450 spectrophotometer (Shimazu, Japan). Zeta potential measurements were performed using a Zetasizer Nano ZS (ZEN3600, Malvern Instruments Ltd., UK). A SU8020 microscope (Japan, Hitachi) was applied to obtain energy-dispersive X-ray spectroscopy (EDS) images. XRD were performed using a BRUCKER D8 ADVANCE (BRUKER, Germany).

Preparation of the Ag/Fe-MOFs endogenous redox mediator

The synthesis of Fe-MOFs was based on our previous work [25]. First, FeCl3·6H2O of 0.187 g and 0.126 g 2-aminoterephthalic acid were dissolved in 15 mL of DMF. Then, the mixture was reacted in a silicone oil bath at

120 °C for 4 h, and 0.2 mL glacial acetic acid was added to this solution after heating for 15 min. After cooling to room temperature, the obtained Fe-MOFs were washed with DMF, ethanol, and ultrapure water followed by centrifugation at 10,000 rpm for 5 min. Finally, the product was dried in a vacuum oven.

The AgNPs were synthesized via the Lee-Meisel method [26]: first, 18 mg $AgNO_3$ was dissolved into 40-mL ultrapure water. Then, the solution was heated to its boiling point. Subsequently, 1.6 mL of sodium citrate (1%) was added into the boiling water. One hour later, the solution was cooled to room temperature, and the gained AgNPs were washed by centrifugation twice at 10,000 rpm, 5 min before dissolution in 40-mL ultrapure water.

Ag/Fe-MOFs nanocomposites were prepared by violently stirring the above Fe-MOFs with AgNPs. First, 1 mg of Fe-MOFs and 1 mg of chitosan were dissolved in 1 mL 1% acetic acid solution. Then, the solution was sonicated in an ultrasonicator for 10 min. After this step, the solution containing Fe-MOFs and chitosan was mixed with a 1-mL AgNP solution and stirred for 12 h at room temperature followed by centrifugation and then washing three times with ultrapure water at 10,000 rpm for 5 min. Finally, the obtained nanocomposites were dissolved into 1-mL ultrapure water.

Preparation of the Mc-Ag/Fe-MOFs composites

First, 30 mg of SH-PEG_{2000}-COOH, 15 mg of EDC, and NHS was dissolved into 2-mL CH_2Cl_2 solution followed by stirring for 12 h. Then, the solution was rotary evaporated at 20 °C. Followed by suction filtration and dissolution of the product in 2 mL ultrapure water, the EDC/NHS-activated SH-PEG-COOH was obtained.

Then, 1 mL of the Ag/Fe-MOFs nanocomposite solution was mixed with 40 μl M-APBA (1 mg/mL) and 40 μl EDC/NHS-activated SH-PEG-COOH (1 mg/mL). Next, the mixture was stirred lightly at 4 °C for 12 h. Finally, the precipitates were collected and washed once and then dispersed in 1 mL of ultrapure water.

Interface modification of the biosensor

A schematic diagram showing the fabrication of the biosensor is presented in Scheme 1. First, the gold electrode was polished by using 0.3 μm and 0.05 μm alumina paste and then rinsed with ultrapure water and ethanol. Then, 8 μl of the SNA (1.0 mg/mL) was incubated onto the gold electrode surface at 37 °C for 2 h. The electrode was then rinsed with ultrapure water. Next, 6 μL of a 0.25 wt% BSA solution was placed onto the modified electrode at room temperature for half an hour in order to block the nonspecific sites.

Measurement procedure

A series of α2,6-sialylated glycan solutions with varying concentrations was added onto the electrode surface and incubated for 2 h at 37 °C. Finally, 10 μL of Mc-Ag/Fe-MOFs solution was coated onto the electrodes for 2 h at 37 °C.

All electrochemical measurements were performed using a conventional three-electrode system with a gold electrode (4.0 mm diameter). The DPV was carried out from − 0.2 to 0.6 V to record current signals in 10.0 mL of PBS (0.1 M, pH 7.2) at room temperature.

Results and discussion

Characterization

TEM, FE-SEM, and zeta potential measurements were used to illustrate the properties of the as-prepared nanomaterials. Figure 1A shows the TEM image of the AgNPs, which show a spherical-like structure with a diameter of 50 ~ 100 nm, similar to the previous report [27]. Figure 1B shows the Fe-SEM image of the Fe-MOFs, which clearly shows a regular octahedron with an average diameter of approximately 300 nm. After treating the Fe-MOFs with chitosan and AgNPs, we found that large amounts of Ag nanoparticles were gathered around the Fe-MOFs (Fig. 1C). To further confirm the Ag/Fe-MOFs composites and the integrated signal probe (Mc-Ag/Fe-MOFs), a zeta potential measurement was used for the determination. As shown in Fig. 1D, when Fe-MOFs successfully combine with AgNPs, the average zeta potential of Ag/Fe-MOFs is changed to 18.8 mV; after it connects to SH-PEG-COOH/M-PABA, the surface potential of the integrated signal is reduced to 1.9 mV, which is similar to the potential of SH-PEG-COOH/M-PABA. These results indicate that the synthesis of Ag/Fe-MOFs was successful and that it can combine with the SH-PEG-COOH/M-PABA. A further demonstration of the formation of Fe-MOFs, Ag/Fe-MOFs by EDS, XRD, and UV-Vis is displayed in Fig. S1 and Fig. S2. These results reveal that Fe-MOFs and Ag/Fe-MOFs were successfully synthesized.

Characteristics of the biosensor fabrication

First, each step of the modification procedure for the gold electrode was characterized by cyclic voltammetry (CV) in 5 mM $[Fe(CN)_6]^{3-/4-}$ solution and the results are shown in Fig. 2A. A pair of peaks were observed on the gold electrode (a). After modifying the surface with SNA, these peaks were found to be decreased because of the antibodies on the electrode surface, the lectin interfering with the electron transfer process between the electrode and $[Fe(CN)_6]^{3-/4-}$ solution (b). After BSA was cast onto the gold electrode to block the possible nonspecific bonding sites, a larger decrease in the CV

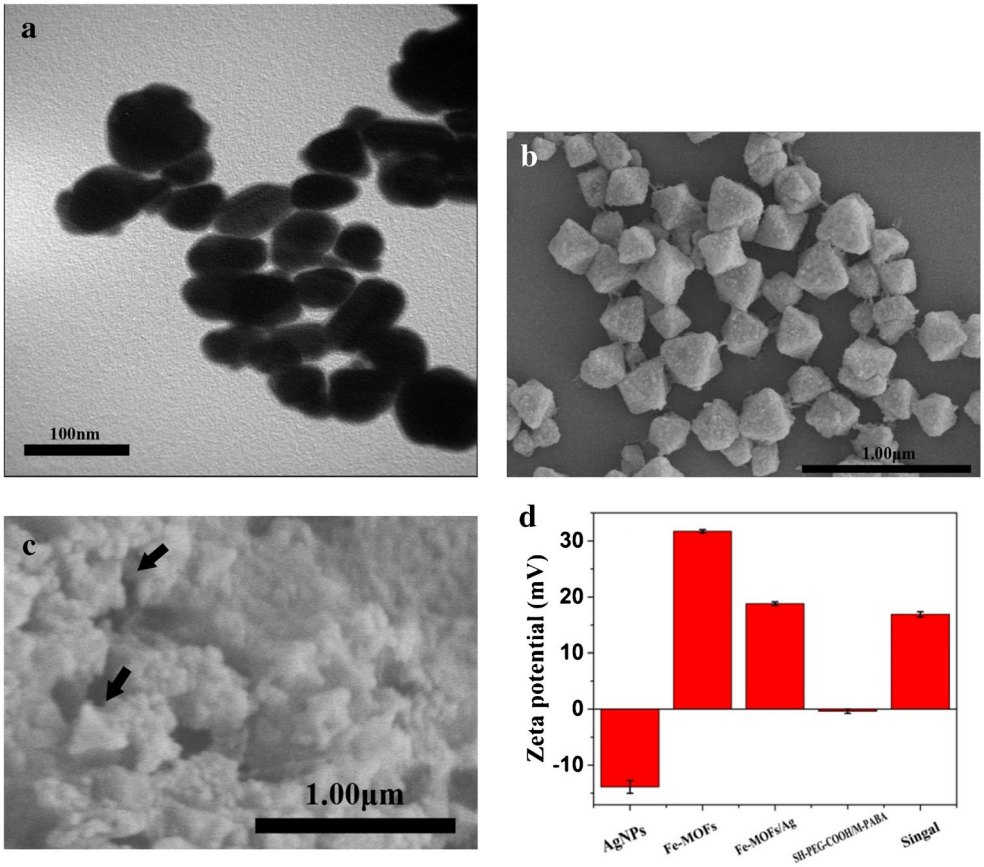

Fig. 1 (A) TEM image of AgNPs; (B) SEM image of Fe-MOFs and (C) Ag/Fe-MOFs: the arrows are referring to individual Ag/Fe-MOFs; (D) zeta potential of AgNPs, Fe-MOFs, Ag/Fe-MOFs, SH-PEG-COOH/M-PABA, and Mc-Ag/Fe-MOFs

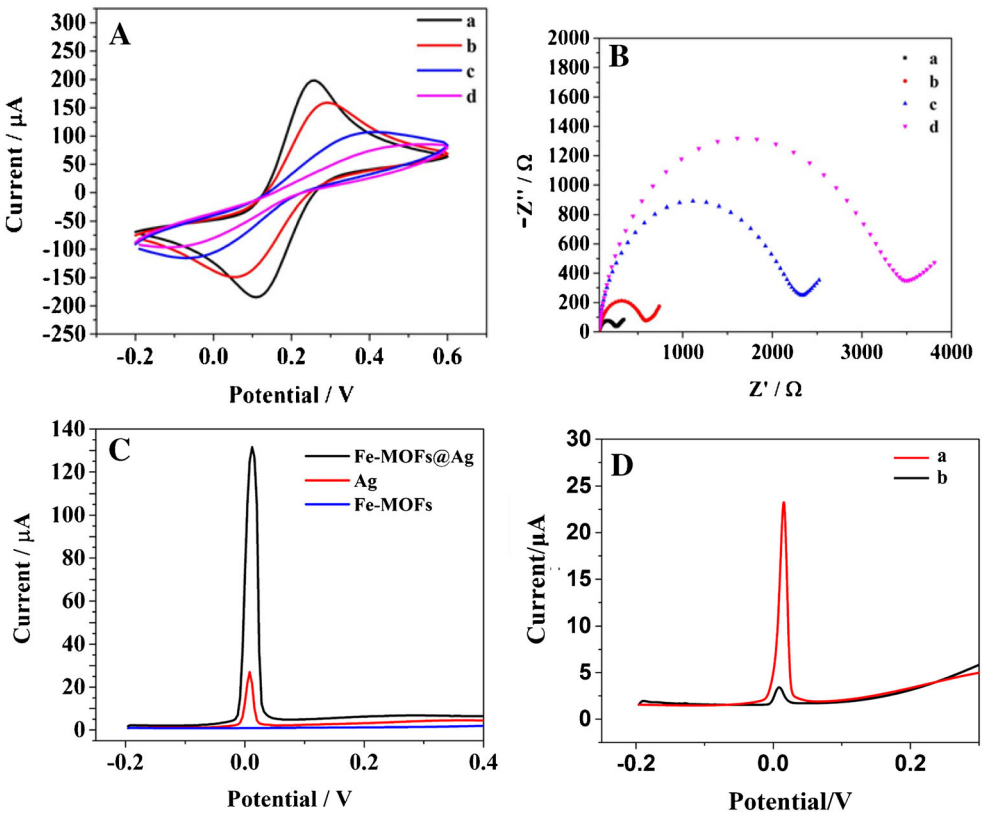

Fig. 2 (A) CV and (B) EIS characterization of the electrodes at various stages of modification in $[Fe(CN)_6]^{3-/4-}$ solution: (a) bare gold electrode, (b) bare gold electrode/SNA, (c) bare gold electrode/SNA/BSA, and (d) bare gold electrode/SNA/BSA/α2,6-sial-Gs; (C) DPV characterization of (a) Ag/Fe-MOFs, (b) Ag, and (c) Fe-MOFs at the bare gold electrode in PBS solution; (D) DPV characterization of the electrode with different signal labels (a) c-Ag/Fe-MOFs and (b) Ag/Fe-MOFs at the same concentration of α2,6-sial-Gsin in PBS solution

peaks was observed (c). Afterwards, the peak for curve d further decreased due to the α2,6-sial-Gs blocking the electrode, demonstrating that the SNA successfully captured the α2,6-sial-Gs. In addition to CV, the EIS method was also applied for further characterization of the biosensor. In the obtained Nyquist diagram, the electron transfer resistance is shown by the diameter of the semicircle found at high frequencies [28]. As shown in Fig. 2B, the gold electrode presented the smallest semicircle (curve a, $R_{ct} = 260\ \Omega$). After incubating with SNA (curve b, $R_{ct} = 590\ \Omega$), the resistance was found to be increased. This resistance was further increased (curve c, $R_{ct} = 2330\ \Omega$) after the biosensor was blocked with BSA, because the BSA hindered the electron transfer. Finally, as a consequence of binding the α2,6-sial-Gs onto the modified electrode surface, a larger increase in the semicircle diameter was observed (curve d, $R_{ct} = 3500\ \Omega$).

To suggest that the Ag/Fe-MOFs endogenous redox mediator has a stronger electrochemical signal than AgNPs, and that the Fe-MOFs have no signal response, DPVs for different gold electrodes modified by using the same amount of Fe-MOFs, Ag, and Ag/Fe-MOFs in pH 7.2 PBS were compared, as shown in Fig. 2C. These results show that the silver current was increased due to Fe-MOFs, while the single Fe-MOFs showed no oxidation current peak.

Finally, to prove that the SH-PEG-COOH-functionalized Ag/Fe-MOFs (c-Ag/Fe-MOFs) have a superior binding ability to that of the α2,6-sial-Gs catcher compared to Ag/Fe-MOFs, a DPV measurement in 10-mL PBS solution was used to detect the current response for the same α2,6-sial-Gs concentration with different signal probes (Ag/Fe-MOFs or c-Ag/Fe-MOFs). As shown in Fig. 2D, the current peak for c-Ag/Fe-MOFs (curve a) was found to be obviously higher than that for the Ag/Fe-MOFs (curve b), indicating that the c-Ag/Fe-MOFs have a better linking ability toward the biological catchers.

Optimization of the experimental condition

To improve the analytical performance of the described method, several conditions were selected for further investigation, such as (a) incubation time for SNA; (b) volume of SNA; (c) incubation times for α2,6-sial-Gs; and (d) pH of the PBS solution. Various working electrodes were used for the detection in different conditions. These results are shown in Fig. S4.

The incubation time of the SNA plays an essential role in influencing the performance of the biosensor by dictating the amount of SNA fixed on the gold electrode surface. As shown in Fig. S4A, the current change increased with the incubation time from 1 to 2 h and barely increased further after reaching a maximum value at 2 h. At this moment, the amount of SNA fixed on the gold electrode reached its maximum. Hence, 2 h was considered as the optimal incubation time for SNA.

The incubation SNA concentration is also an extremely important factor that can influence the amount of SNA loaded onto the electrode surface. The effect of the lectin concentration on the response of the biosensor was investigated by using 0.05 mg/mL, 0.5 mg/mL, 1 mg/mL, and 1 mg/mL of SNA. The results (Fig. S4B) indicate that the observed current change increased from 0.05 to 1 mg/mL. When the concentration was larger than 1 mg/mL, the current remained stable. Therefore, 1 mg/mL was selected as the optimal SNA incubation concentration.

In addition, the incubation time for the α2,6-sial-Gs was tested. It was found that the current change increased with time from 0.5 to 2 h. The current change remained steady after 2 h (Fig. S4C), indicating that the specific binding of α2,6-sial-Gs and lectin reached an optimum at 2 h. Hence, an α2,6-sial-Gs incubation time of 2 h was the optimal condition.

Finally, the pH of the PBS is an important parameter for the performance of the biosensor. A highly acidic or alkaline environment may result in damage to the linkage of the α2,6-sial-Gs and lectin. The modified electrode was tested in 10-mL PBS with pH values varying from 5.0 to 9.0, as shown in Fig. S4D. The current response was found to first increase from pH 4.0 to 7.2 and then obviously decrease at pH values higher than 7.2. The maximum point was observed at 7.2, which is close to the protein isoelectric point, as reported in previous work [29].

Detection and analysis of α2,6-sial-Gs

To explore the quantitative range and sensitivity of the prepared biosensor, the relationship between α2,6-sial-Gs concentration and the oxidation peak current for AgNPs in PBS was investigated under the optimal conditions (Fig. 3). As presented in Fig. 3A, the DPV current peak for the biosensor

Table 1 Comparison of other methods of α2,6-sial-Gs detection

Type of affinity assay	Detection method	Liner range	Detection limit	References
GCE/GO-PB-PTC-NH3/GNPs/SNA/α2,6-sial-Gs	DPV	0.1 pg mL^{-1} ~ 500 ng mL^{-1}	30 fg mL^{-1}	[30]
GCE/MPF6/rGO-TEPA-BMI/DpAuPtNPs/SNA/α2,6-sial-Gs	DPV	10 fg mL^{-1} ~ 1 μg mL^{-1}	3 fg mL^{-1}	[31]
GCE/AuNRs-SA/bio-SNA/BSA/α2,6-sial-Gs/SWCNHs/s-PtNC	i-t	10 fg mL^{-1} ~ 5 μg mL^{-1}	0.69 fg mL^{-1}	[1]
Gold electrode/SNA/α2,6-sial-Gs/M-PABA/s-Ag/Fe-MOFs	DPV	1 fg mL^{-1} ~ 1 ng mL^{-1}	0.09 fg mL^{-1}	This work

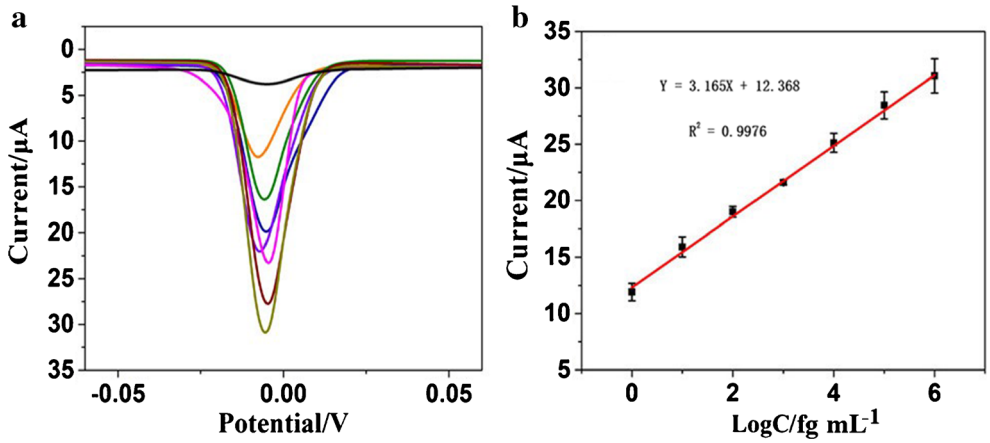

Fig. 3 (A) Differential pulse voltammetry response of the proposed electrochemical biosensor for the determination of different concentrations of α2,6-sial-Gs: (a) 0 fg mL^{-1}; (b) 1 fg mL^{-1}; (c) 10 fg mL^{-1}; (d) 100 fg mL^{-1}; (e) 1 pg mL^{-1}; (f) 10 pg mL^{-1}; (g) 100 pg mL^{-1}; (h) 1 ng mL^{-1}. (B) The calibration curve for the sandwich-type biosensor for different concentrations of α2,6-sial-Gs

gradually increases with increasing α2,6-sial-Gs target concentration in 10 mL of PBS. This result shows that the variation in the current is connected to the quantity of α2,6-sial-Gs that is captured. In the range of 1 fg mL^{-1} to 1 ng mL^{-1}, the calibration plot (Fig. 3B) showed a good linear relationship. This relationship can be described by a linear regression equation expressed as $Y = 3.165\log([\alpha 2,6\text{-sial-Gs}]\ (\text{fg mL}^{-1})) + 12.368$, with a correlation coefficient of 0.9976. The limit of detection was found to reach 0.09 fg mL^{-1}, which is defined as $DL = 3SB/m$, where SB is the standard deviation of a blank and m is the calibration curve slope. Compared with the previously reported sensor used for the detection of α2,6-sial-Gs shown in Table 1, the biosensor achieved a lower detection limit by only using a single amplification system with Fe-MOFs. As a result, a novel and ultrasensitive biosensor for α2,6-sial-Gs detection was established.

Specificity and stability of the biosensor

The specificity of detection is a significant property for analytical methods. To assess the specificity of the sandwich-type biosensor, different interfering substances were selected to compare with the α2,6-sial-Gs (10 pg mL^{-1}) and mixture sample, such as Neu5Ac α(2–3)Gal β MP glycoside (α2,3-sial-Gs) (1 ng mL^{-1}), glucose (1 ng mL^{-1}), AA (1 ng mL^{-1}), and L-cysteine (1 ng mL^{-1}). Except for α2,6-sial-Gs and the mixture, the amount of the other 4 kinds of substances were found to be 100 times higher than α2,6-sial-Gs; however, these substances did not interfere with the detection, with a very weak current peak observed (Fig. 4A). This result demonstrates that the current peak response arises from the specific recognition of α2,6-sial-Gs and SNA, indicating the high specificity of the sandwich-type biosensor.

To prove that the electrochemical biosensor can be selective to some typical interference in serum, we also detected three other interfering substances that are common in serum and which have a chemical structure that is similar to that of α 2,6-sialylated glycans. The interfering substances include chondroitin sulfate (1 ng mL^{-1}), heparin (1 ng mL^{-1}), and hyaluronic acid (17KD, 1 ng mL^{-1}). As shown in Fig. S2, even at tenfold higher concentrations than that of α 2,6-sialylated glycans (10 pg mL^{-1}), the current response is significantly lower than that for α 2,6-sialylated glycans, indicating that the selectivity for typical interference in serum for the biosensor is acceptable.

Stability is another important factor for determining the performance of the biosensor. After storing, the fabricated

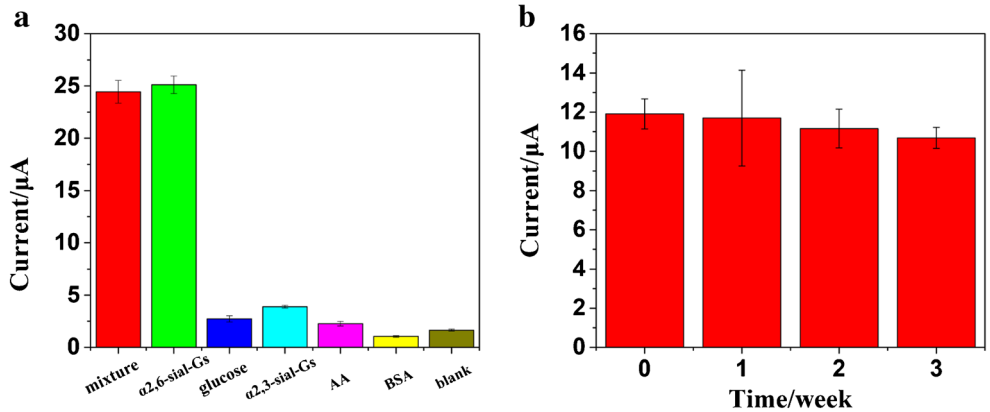

Fig. 4 (A) Specificity of the sandwich-type biosensor toward 10 pg mL^{-1} of mixture, α2,6-sial-Gs, 1 ng mL^{-1} of glucose, α2,3-sial-Gs, AA, BSA, and blank control. (B) The stability study for the biosensor

Table 2 Recoveries of α2,6-sial-Gs in human serum samples with the constructed biosensors

Samples	Added α2,6-*sial-Gs* (pg mL^{-1})	Founded α2,6-sial-Gs (pg mL^{-1})	Recovery (%, $n = 3$)	RSD (%, $n = 3$)
Sample-1	1.00×10^{-3}	0.830×10^{-3}	82.8	5.62
Sample-2	1.00×10^{3}	0.955×10^{3}	95.5	4.28

biosensors at 4 °C for 21 days, the corresponding DPV current peak was found to be decreased by only 1.8% of its initial current in the first week (Fig. 4B). The change in current was also found to remain at 89.67% compared to the original current after 3 weeks.

Serum simple assay

To verify the applicability of the fabricated biosensor for biological samples, the prepared biosensor was used to detect the recoveries of α2,6-sial-Gs in human diluted serum sample by using standard addition methods. The recovery rates were found to be 82.79 ~ 95.5%, as shown in Table 2, with RSDs of no more than 5.165%. These results also demonstrated that the purposed biosensor can be effectively applied to the detection of α2,6-sial-Gs in human serum and its clinical application.

Conclusions

In general, an electrochemical biosensor was constructed for determination of α2,6-sial-Gs based on Mc-Ag/Fe-MOFs as a novel signal probe. The affinity biosensor presented some advantages, including a rapid method for α2,6-sial-Gs detection, good selectivity, and sensitive and low detection limit. The determination of α2,6-sial-Gs in human serum samples with satisfactory results was also obtained. In addition, a novel endogenous redox mediator, Ag/Fe-MOFs, was obtained by combining the AgNPs with Fe-MOFs. Moreover, after modifying Ag/Fe-MOFs with SH-PEG-COOH, c-Ag/Fe-MOFs was synthesized for the first time. This surface modification strategy affords numerous biocatchers a powerful ability to combine with metal-organic frameworks; thus, more biomarkers identified by kinds of biocatchers can be detected. Based on this extensive properties of combination, c-Ag/Fe-MOFs holds great potential for detection of all other biomarkers in clinical diagnostics.

Acknowledgments We are grateful for the financial support from Chongqing precision medical key technology research and development and demonstration projects (cstc2016shms-ztzx0042).

Compliance with ethical standards

Conflict of interest The authors declare that they have no competing interest.

References

1. Li J, He J, Zhang C, Chen J, Mao W, Yu C (2019) Dual-type responsive electrochemical biosensor for the detection of alpha2, 6-sialylated glycans based on AuNRs-SA coupled with c-SWCNHs/S-PtNC nanocomposites signal amplification. Biosens Bioelectron 130:166–173
2. Dall'olio F, Malagolini N, Di Stefano G et al (1989) Increased CMP-NeuAc:Gal beta 1,4GlcNAc-R alpha 2,6 sialyltransferase activity in human colorectal cancer tissues. Int J Cancer 44:434–439
3. Recchi MA, Hebbar M, Hornez L, Harduin-Lepers A, Peyrat JP, Delannoy P (1998) Multiplex reverse transcription polymerase chain reaction assessment of sialyltransferase expression in human breast cancer. Cancer Res 58:4066–4070
4. Wang PH, Li YF, Juang CM et al (2001) Altered mRNA expression of sialyltransferase in squamous cell carcinomas of the cervix. Gynecol Onclo 83:121–127
5. Zhao Y, Li Y, Ma H, Dong W, Zhou H, Song X, Zhang J, Jia L (2014) Modification of sialylation mediates the invasive properties and chemosensitivity of human hepatocellular carcinoma. Mol Cell Proteomics 13:520–536
6. Harvey DJ (2011) Derivatization of carbohydrates for analysis by chromatography; electrophoresis and mass spectrometry. J Chromatgr B Analyt Technol Biomed Life Sci 879:1196–1225
7. Patil SA, Bshara W, Morrison C, Chandrasekaran EV, Matta KL, Neelamegham S (2014) Overexpression of alpha2,3sialyl T-antigen in breast cancer determined by miniaturized glycosyltransferase assays and confirmed using tissue microarray immunohistochemical analysis. Glycoconj J 31:509–521
8. Tothill IE (2009) Biosensors for cancer markers diagnosis. Semin Cell Dev Biol 20:55–62
9. Yang B, Zhang S, Fang X, Kong J (2019) Double signal amplification strategy for ultrasensitive electrochemical biosensor based on nuclease and quantum dot-DNA nanocomposites in the detection of breast cancer 1 gene mutation. Biosens Bioelectron 142: 111544
10. Liu YL, Zhao XJ, Yang XX, Li YF (2013) A nanosized metal-organic framework of Fe-MIL-88NH(2) as a novel peroxidase mimic used for colorimetric detection of glucose. Analyst 138: 4526–4531
11. Cao J, Li X, Tian H (2019) Metal-organic framework (MOF)-based drug delivery. Curr Med Chem 21:5949–5969
12. Xie S, Ye J, Yuan Y, Chai Y, Yuan R (2015) A multifunctional hemin@metal-organic framework and its application to construct an electrochemical aptasensor for thrombin detection. Nanoscale 7: 18232–18238
13. Baghayeri M, Ghanei-Motlagh M, Tayebee R, Fayazi M, Narenji F (2020) Application of graphene/zinc-based metal-organic framework nanocomposite for electrochemical sensing of as(III) in water resources. Anal Chim Acta 1099:60–67
14. Zhang C, He J, Zhang Y, Chen J, Zhao Y, Niu Y, Yu C (2018) Cerium dioxide-doped carboxyl fullerene as novel nanoprobe and catalyst in electrochemical biosensor for amperometric detection of the CYP2C19*2 allele in human serum. Biosens Bioelectron 102: 94–100

15. Qiao X, Xia F, Tian D (2019) Ultrasensitive "signal-on" electrochemical aptasensor for assay of acetamiprid residues based on copper-centered metal-organic frameworks. Anal Chim Acta 1050:51–59
16. Chen J, Yu C, Zhao Y (2017) A novel non-invasive detection method for the FGFR3 gene mutation in maternal plasma for a fetal achondroplasia diagnosis based on signal amplification by hemin-MOFs/PtNPs. Biosens Bioelectron 91:892–899
17. Zhao Y, Yang Y, Cui L (2018) Electroactive Au@Ag nanoparticles driven electrochemical sensor for endogenous H(2)S detection. Biosens Bioelectron 117:53–59
18. Benton EN, Marpu SB, Omary MA (2019) Ratiometric phosphorescent silver sensor: detection and quantification of free silver ions within silver nanoparticles. ACS Appl Mater Interfaces 11:15038–15043
19. Saleh T, Ahmed E, Yu L, Kwak HH, Kang BJ, Park KM, Choi KY, Kim BM, Kang KS, Woo HM (2019) Characterization of silver nanoparticle-modified decellularized rat esophagus for esophageal tissue engineering: structural properties and biocompatibility. J Biosci Bioeng 128:613–621
20. Liu R, Yu T, Shi Z, Wang Z (2016) The preparation of metal-organic frameworks and their biomedical application. Int J Nanomedicine 11:1187–1200
21. Baghayeri M, Veisi H, Ghanei-Motlagh M (2017) Amperometric glucose biosensor based on immobilization of glucose oxidase on a magnetic glassy carbon electrode modified with a novel magnetic nanocomposite. Sensor Actuat B-Chem 249:321–330
22. Baghayeri M, Veisi H, Farhadi S, Beitollahi H, Maleki B (2018) Ag nanoparticles decorated Fe_3O_4/chitosan nanocomposite: synthesis, characterization and application toward electrochemical sensing of hydrogen peroxide. J Iran Chem Soc 15:1015–1022
23. Kong W, Guo X, Jing M et al (2019) Highly sensitive photoelectrochemical detection of bleomycin based on au/WS2 nanorod array as signal matrix and Ag/ZnMOF nanozyme as multifunctional amplifier. Biosens Bioelectron 15(150):111875
24. Kreno LE, Leong K, Farha OK, Allendorf M, van Duyne RP, Hupp JT (2012) Metal-organic framework materials as chemical sensors. Chem Rev 112:1105–1125
25. Chen J, Yu C, Zhao Y, Niu Y, Zhang L, Yu Y, Wu J, He J (2017) A novel non-invasive detection method for the FGFR3 gene mutation in maternal plasma for a fetal achondroplasia diagnosis based on signal amplification by hemin-MOFs/PtNPs. Biosens Bioelectron 91:892–899
26. Wang Y, Zhao G, Zhang Y, Pang X, Cao W, du B, Wei Q (2018) Sandwich-type electrochemical immunosensor for CEA detection based on Ag/MoS2@Fe3O4 and an analogous ELISA method with total internal reflection microscopy. Sensor Actuat B-Chem 266:561–569
27. Shankar SS, Rai A, Ahmad A, Sastry M (2004) Rapid synthesis of Au, Ag, and bimetallic Au core-Ag shell nanoparticles using neem (Azadirachta indica) leaf broth. J Colloid Interface Sci 275:496–502
28. Yuan Q, He J, Niu Y, Chen J, Zhao Y, Zhang Y, Yu C (2018) Sandwich-type biosensor for the detection of alpha2,3-sialylated glycans based on fullerene-palladium-platinum alloy and 4-mercaptophenylboronic acid nanoparticle hybrids coupled with Au-methylene blue-MAL signal amplification. Biosens Bioelectron 102:321–327
29. Arkan E, Saber R, Karimi Z, Shamsipur M (2015) A novel antibody-antigen based impedimetric immunosensor for low level detection of HER2 in serum samples of breast cancer patients via modification of a gold nanoparticles decorated multiwall carbon nanotube-ionic liquid electrode. Anal Chim Acta 874:66–74
30. Gao L, He J, Xu W, Zhang J, Hui J, Guo Y, Li W, Yu C (2014) Ultrasensitive electrochemical biosensor based on graphite oxide, Prussian blue, and PTC-NH2 for the detection of alpha2,6-sialylated glycans in human serum. Biosens Bioelectron 62:79–83
31. Li Y, He J, Niu Y, Yu C (2015) Ultrasensitive electrochemical biosensor based on reduced graphene oxide-tetraethylene pentamine-BMIMPF6 hybrids for the detection of alpha2,6-sialylated glycans in human serum. Biosens Bioelectron 74:953–959